

# Structural and surface characterization of undoped ZnO and Cu doped ZnO using sol–gel spin coating method

Nur Hasyimah Hashim<sup>1</sup> · Shanmugam Subramani<sup>1</sup> · Mutharasu Devarajan<sup>1</sup> · Abdul Razak Ibrahim<sup>1</sup>

Received: 20 August 2015 / Accepted: 7 December 2015 / Published online: 28 December 2015  
© Springer Science+Business Media New York 2015

**Abstract** In this work, the preparation of undoped and Cu doped ZnO thin films by sol–gel spin coating method was reported. Undoped ZnO was deposited on aluminium and silicone substrates followed by annealing at three different temperatures (350, 450 and 550 °C) and optimized the annealing temperature of ZnO thin film for Cu doping on Al substrates as 550 °C. The structural properties of undoped ZnO showed hexagonal crystal structure. The structural properties such as crystallite size, orientation and surface properties of annealed thin film samples at various temperatures are discussed. Undoped ZnO sol–gel for peak (002) give crystallite size within range 0.1–0.4 nm for Al and Si substrates. The observation was showed that the surface becomes smoother and grain size was increased for higher annealing temperature. For Cu doped ZnO, various concentration of Cu doping (0.03 M:Cu, 0.05 M:Cu and 0.07 M:Cu) was deposited on Al substrate which then undergone 550 °C annealing temperature. The morphological properties of Cu doped ZnO were investigated using FESEM where the surface becomes smooth with increasing doping concentration while atomic force microscopy showed anomalous results for surface roughness and particle size. Optical properties from Fourier transform infrared spectrometer showed the presence of functional groups and the absorption range from the peak. It was revealed that the influence of Cu doping to ZnO where the changes can be seen from surface morphology and structural properties. In addition to that annealing

treatment also played role in improving the crystallization process.

## 1 Introduction

Study on semiconductor in films is the one of important field in materials science due to their performance in electrical and optical properties especially in optoelectronic devices. A wide band gap (3.37 eV) and large exciton binding energy (60 meV) at room temperature have established ZnO as promising materials that suited for UV light emitting diodes, laser diode, light emitting diodes and even transparent electrodes in solar cells. ZnO has been proposed to be a more promising UV emitting phosphor than GaN because of its larger exciton binding energy [1]. ZnO is transparent to visible light and can be made highly conductive by doping. ZnO has a long history of usage for pigments and protective coatings on metals. Many growth methods for thin film preparation have been used for ZnO thin film synthesis such as molecular beam epitaxy (MBE) [2], metal–organic chemical vapor-deposition [3] and sputtering deposition where ZnO thin film with high quality and uniformity is required. Nevertheless, highly expensive and sophisticated processes are mainly used which ignore economical cost concerns. Sol–gel spin coating is one of methods that involve low cost equipment and raw material where the properties of the ZnO films will correlate with the sol–gel preparation conditions and parameters. Bacaksiz [4] reported that ZnO films is polycrystalline and have a hexagonal wurtzite crystal structure while Ashikin et al. [5] stated from the results that all sol–gel fabricated ZnO films have sharp and narrow diffraction peaks which indicating that the materials exhibit high crystallinity. Other than that, FWHM of ZnO thin film decreases with increasing annealing temperature which can

✉ Nur Hasyimah Hashim  
nurhasyimah92@gmail.com

<sup>1</sup> Nano Optoelectronics Research Laboratory, School of Physics, Universiti Sains Malaysia (USM), 11800 Minden, Pulau Pinang, Malaysia

be attributed to the coalescences of grains at higher annealing temperature and indicate a better crystallization [6]. Dejam [7] reported crystallite size and peak position (002) of ZnO is increased by increasing annealing temperature that possible to state the post annealing led to the evaporation of trapped oxygen atoms in vacancies which is resulted to increase of crystalline size. Preferential crystal orientation of (002) was more likely to grow at lower temperatures which could signify that their surface free energy but for annealed ZnO film at 500 °C, due to the increment of free surface energy, other crystal orientation were also noticed. The annealing temperature enhances the crystal quality by crystallization and reduces the impurities/defects without changing hexagonal wurtzite structure.

Many attempts have been made or modify the properties of ZnO such as adding dopants into ZnO in order to increase the multifunctionality by change the phase of the material and hence the structural defects. The ZnO has wurtzite crystal structure in which zinc atoms are arranged in hexagonal close packed lattice therefore, its structure is relatively open with all the octahedral and half of the tetrahedral sites empty. Thus, it was easy to incorporate dopants in the zinc oxide lattice. Among various dopants, transition metal doped ZnO results with an increased in electrical conductivity and modification of the energy band of the ZnO thin film [8]. Cu element is one of selective transition metal that has almost equal ionic radius (0.73 Å) to the ionic radius of  $Zn^{2+}$  (0.74 Å), this similar electronic shell structure between Cu and Zn has determined for it to be most suitable doping materials. All coefficient measurements have shown that number of carriers is reduced by Cu doping at room temperature since some of the n-type ZnO electrons occupies empty lower energy  $3d$  Cu states leading to  $Cu^+$  ions [9]. The FWHM and height of (002) peak increased with the increase of the Cu-doped concentration. The comprehensive analysis showed that the crystallization quality of the sample was deteriorated gradually with the increase of Cu-doped concentration.

In this effort, undoped ZnO thin film is deposited on Al and Si substrates by spin coating process followed by annealing to optimize the annealing temperature for Cu doped ZnO thin film on Al substrates. The structural and surface properties of undoped and Cu doped ZnO thin film are studied by XRD and SEM and AFM analysis and the results are reported and discussed here. In addition, the optical properties of Cu doped ZnO thin film are studied.

## 2 Experimental details

Undoped ZnO and Cu doped thin films were prepared by sol–gel method on Si (111) and Al substrates AL 104529 from Advent Research Material. Si substrates were cleaned

using chemical method by RCA cleaning while Al substrates were cleaned using soap oil followed by ultrasonic cleaner. The basic solutions which is ZnO solution were prepared by dissolving zinc acetate dihydrate [ $Zn(CH_3COO)_2 \cdot 2H_2O$ ] in isopropanol (IPA) with continuous stirring using magnetic stirrer at temperature 60 °C on magnetic hot plate. Since the solubility of zinc acetate in isopropanol is very poor then, methanolamine (MEA) was slowly added for better dissolution of the mixture. The mixture was stirred at 60 °C for 15 min and obtains a clear and homogenous solution. Finally, a solution with a concentration of 0.4 mol/l was obtained.

To produce Cu doped ZnO, copper (II) acetate monohydrate was selected as a source material. In order to synthesize the solution, 0.4 M Zinc acetate was dissolved in 20 ml IPA followed by the addition of copper (II) acetate under continuous stirring by using magnetic stirrer. After that, MEA was added to get clear solution. In order to deposit the film on the substrates, spin coating unit was used and dried substrates were put on the center of spin coater using double sided tape to hold the substrate at center during coating process. Two drops of prepared sol–gel solution were put at center of substrate by plastic dropper. The rotating disc speed was maintained with 3000 rpm for 30 s for undoped and doped ZnO. The coating cycles for each substrate was 20 layers. Drying time was set as 3 min at 200 °C for all samples. Finally, all samples were undergone annealing treatment using nitrogen gas at 10 sccm flow rate. The annealing process was carried out at 350, 450 and 550 °C for about 1 h.

Structural properties of the samples were analyzed using XRD (X'pert = PRO, Phillips, Netherlands) with  $CuK\alpha$  radiation ( $\lambda = 1.5406 \text{ \AA}$ ) with scanning range between  $2\theta = 20^\circ$  and  $65^\circ$ . The surface morphology of undoped and doped ZnO was tested by atomic force microscope (AFM) using tapping mode by which the surface roughness and particle size were also measured. Field emission scanning electron microscopy (FESEM) was utilized to analysis the surface features using 100 kx magnification. In addition to the above, FTIR analysis was also carried out for the investigation on the chemical composition of the samples.

## 3 Results and discussion

### 3.1 Structural and morphological characterizations of undoped ZnO

The XRD spectra of undoped ZnO sample on aluminium (Al) and silicone (Si) substrates are recorded as shown in Fig. 1a, b, respectively. It shows the behavior of undoped ZnO on various annealing temperature from 350 to 550 °C.

From the XRD analysis, it was confirmed that the XRD pattern matches well with crystallized wurtzite structure of ZnO from JCPDS data card. For ZnO coated on Al substrates (Fig. 1a), peaks ZnO belonging to (100), (002), (101) and (102) planes were observed for ZnO phases. From Fig. 1a, strong peak (002) of wurtzite ZnO at  $34.451^\circ$  was noticed while two additional diffraction peaks are also observed at angle  $38.552^\circ$  and  $44.799^\circ$  for all annealing temperatures. These extra peaks are indexed as Al substrates (JCPDS Card No.: 01-075-0841). For Si thin films, strongest detected (hkl) was observed at  $2\theta$  value of  $34.508^\circ$  which correspond to lattice plane with (111) oriented ZnO all annealed temperatures. When annealing temperature increases from 350 to 550 °C, it was noticed that the XRD peak related to (002) shifted orientation was slightly towards left from  $34.520^\circ$  to  $34.451^\circ$  for Al

substrates (Fig. 1a) and shifted to higher angle from  $34.394^\circ$  to  $34.508^\circ$  for Si substrates (Fig. 1b). As reported by Lauren, peak shifting in XRD spectra is possible due to release of intrinsic strain as a result of annealing process [10]. Other than that, it was also observed that an extra peak related to ZnO (100) orientation was noticed from Si substrate when temperature increased.

Annealing process influences more on the structural properties and hence the position and FWHM of the respective peak will change with respect to the annealing temperatures. When the material treated at low annealing temperature or as grown condition, the atom gets less energy and thus the surface mobility of atoms is low which gives defects to ZnO lattice. As annealing temperature increases, atoms are gaining sufficient kinetic energy and acquired surface mobility to occupy stable positions inside

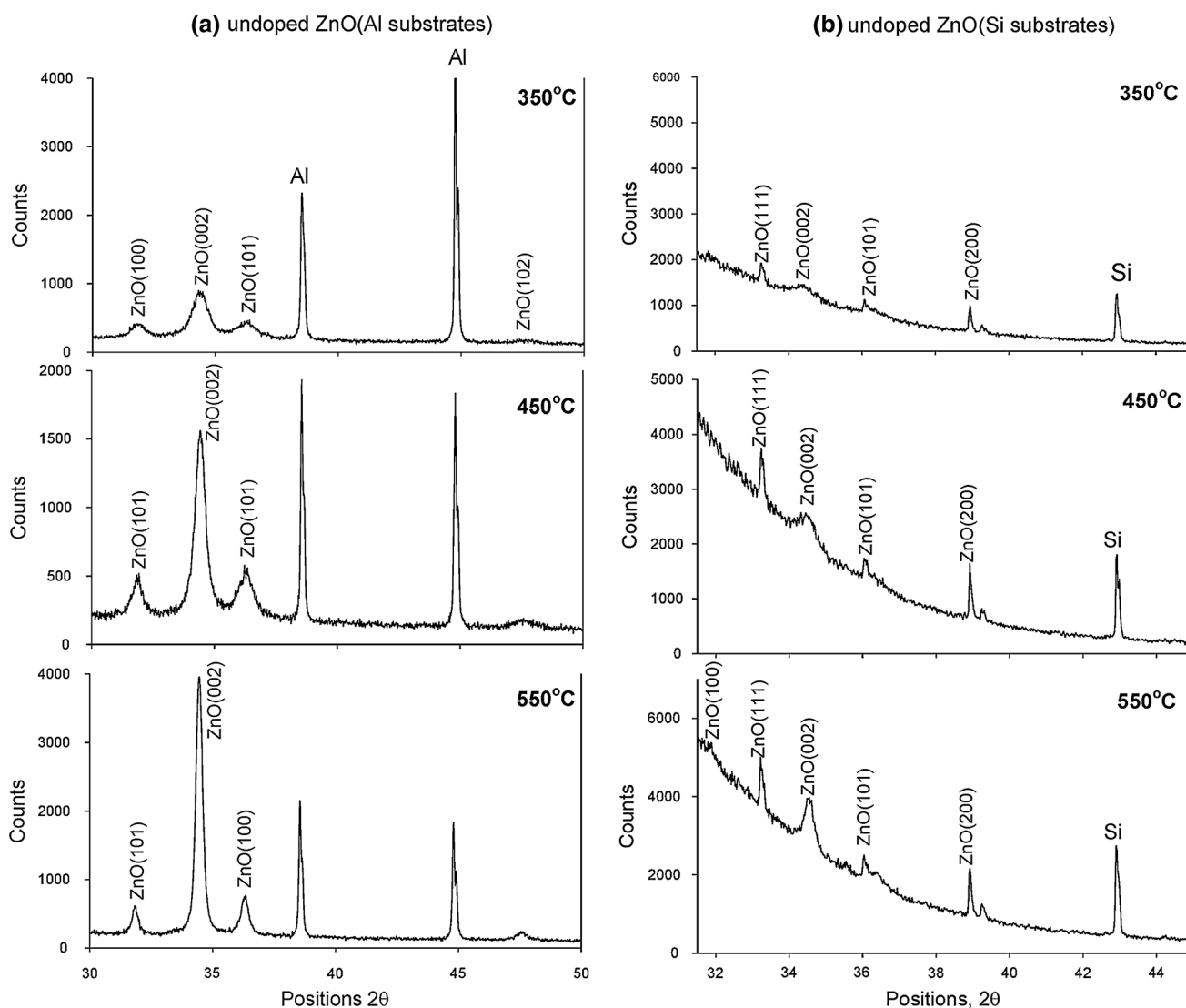


**Fig. 1** XRD spectra of undoped ZnO thin film on **a** Al substrate and **b** Si substrate for different annealed temperature

ZnO crystals [11]. Next, increase in crystallite size during annealing process can be understood with merging process from the particles that induced from thermal treatment. The dangling bonds related to zinc and oxygen defects in the grain boundaries favor the merging process to form larger crystallite size while increasing the annealing temperature [12]. In order to investigate the effect of annealing on crystalline quality, the crystallite size (D) could be calculated by Scherrer’s formula:

$$D = \frac{0.94\lambda}{\beta \cos \theta}$$

where D is crystallite size,  $\lambda$  (=1.5409 Å) is the wavelength of the X-ray source,  $\beta$  is the broadening of diffraction line measured at half of its maximum intensity in radians FWHM and  $\theta$  is the angle of diffraction peak. The calculated crystallite size from the XRD data are presented in Table 1.

The XRD analysis revealed there is an increment for crystallite size where it is sensitive to the annealing temperature which can be seen some peak got increase in crystallite size. It is happened because of high annealing temperature will provide energy to crystallites in order to gain enough energy for orientation of proper equilibrium sites which resulting in the improvement of crystallinity and degree of orientation of the ZnO films. Ashokkumar [13] reported that annealing temperature plays key role in crystallization by moving interstitial atoms towards corresponding vacancies. Increment in annealing temperature moves more and more interstitial atom to its lattice site which reduces the level of defects for better crystallization. Kuo et al. [14] observed improvement in crystallinity and ZnO films with the increase of annealing temperature. Besides that, Kuo reported clearly that not only the (002) peak intensity increases but also the full-width at half maximum (FWHM) for the (002) peak decreases with increasing annealing temperatures.

FESEM results were used to inspect the surfaces of as-grown ZnO thin films and the effect of annealing on the microstructures. Besides, it can be seen that the surface topography of each substrate become finer and smooth

when annealing temperature increases. Figure 2 shows FESEM images of ZnO thin film on Si substrates and Al substrates for different annealed temperature (350, 450 and 550 °C). On close inspection of FESEM image from Fig. 2a until Fig. 2f, the grain size and porous decrease with increment of annealing temperature where each samples show homogenous particle distribution and smooth surface of thin films. As the annealing temperature increases, the atoms obtain higher energy and hence the crystalline defects densities decreases, which contribute to the film’s growth which result in the form of smooth and uniform surfaces of the ZnO thin films. It demonstrates that the quality of ZnO thin films has improved due to re-distribution of crystalline grain island, which will form into good crystalline surface [15]. Referring to data from XRD, crystallite size become bigger as annealing temperature increase but surface morphology show opposite result where the surface become smooth and fine when reached 550 °C. Next, to study the influence of doping into ZnO properties when it is deposited on metal substrate, subsequent experiment was conducted by coating doped ZnO thin film on Al substrate. Cu has been chosen as a dopant and prepared Cu doped ZnO thin film by spin coating process. Structural and surface morphology were discussed for Cu doped ZnO.

### 3.2 Structural characterization of Cu doped ZnO

The undoped ZnO sample annealed at 550 °C was selected for comparison since it was showed good results in both XRD and surface properties. The Cu doped ZnO thin film was also annealed at 500 °C for comparison. Figure 3 shows the XRD pattern of doped ZnO thin films with different Cu concentration deposited on Al substrates which are annealed at 500 °C for 1 h. The Cu concentration in the sample as well as in the results was expressed by mole percent of copper and zinc in sol–gel. For all samples, the XRD patterns was indexed to wurtzite ZnO (JCPDS No.: 01-079-0205) which was also observed by Gadallah et al. [16]. As we observed the diffractive peaks related to (100), (002), (101) orientation of ZnO for our thin films, it is

**Table 1** The data evaluated from XRD of ZnO sol–gel for peak (002) on Al and Si substrates for different annealing

Annealing temperature (°C)	Substrate	Position (2θ)	D-spacing (Å)	FWHM (β)	Crystallite size [D (nm)]
350	Al	34.520	2.598	0.708	0.123
	Si	34.394	2.608	0.779	0.112
450	Al	34.390	2.606	0.443	0.196
	Si	34.505	2.597	0.356	0.244
550	Al	34.451	2.603	0.302	0.288
	Si	34.508	2.591	0.206	0.421

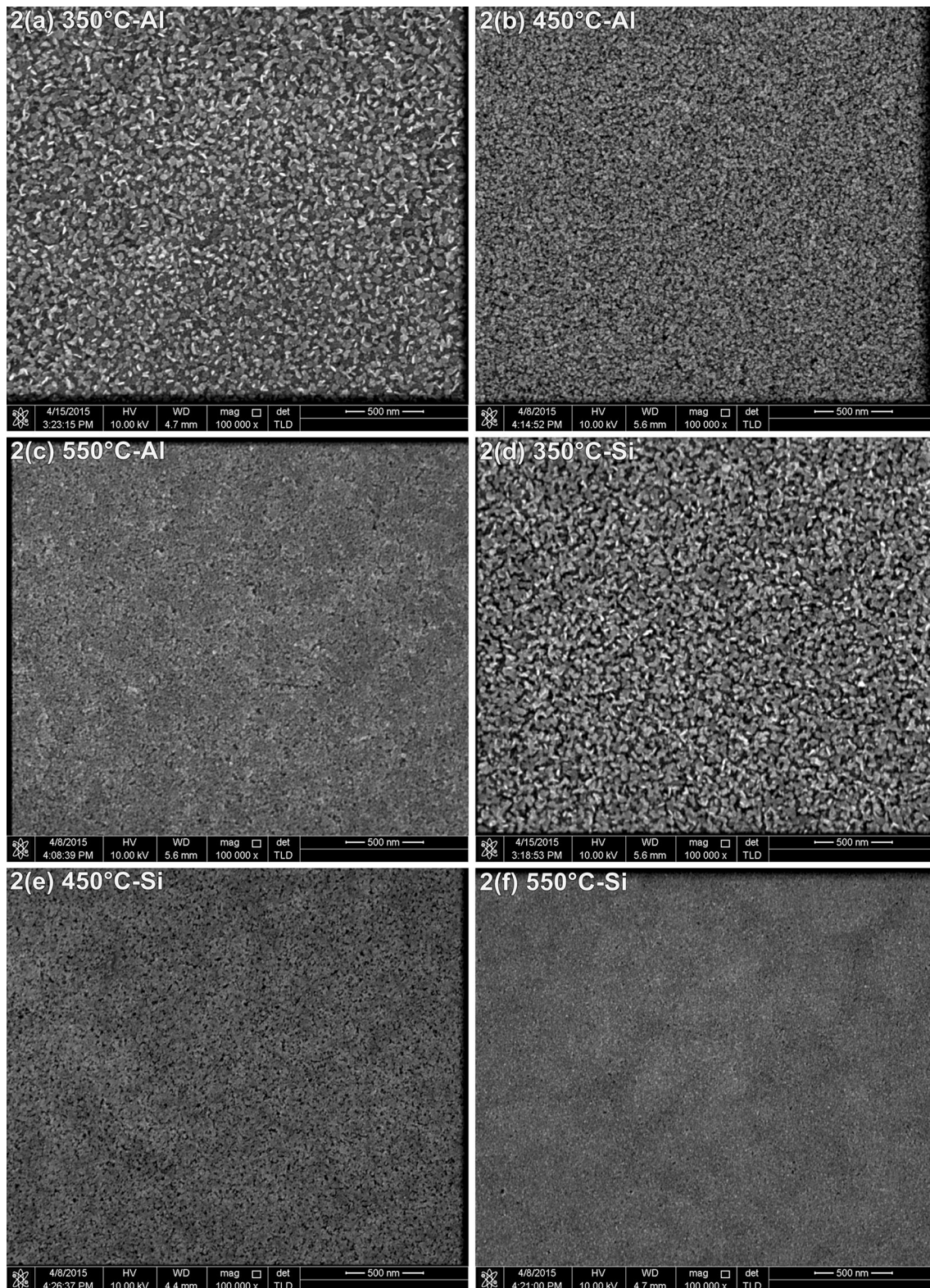


**Fig. 2** FESEM images of undoped ZnO thin film on Al substrates (a–c) and Si substrates (d–f) for different annealed temperature

claimed that the synthesized film is polycrystalline. When compared pure ZnO and Cu doped ZnO, the intensity of (100) oriented peaks increases as the Cu concentration

increases while peak (002) shows opposite result of that both peaks. Peak (002) showed anomalous for intensity as doping concentration increase. Similar observation was

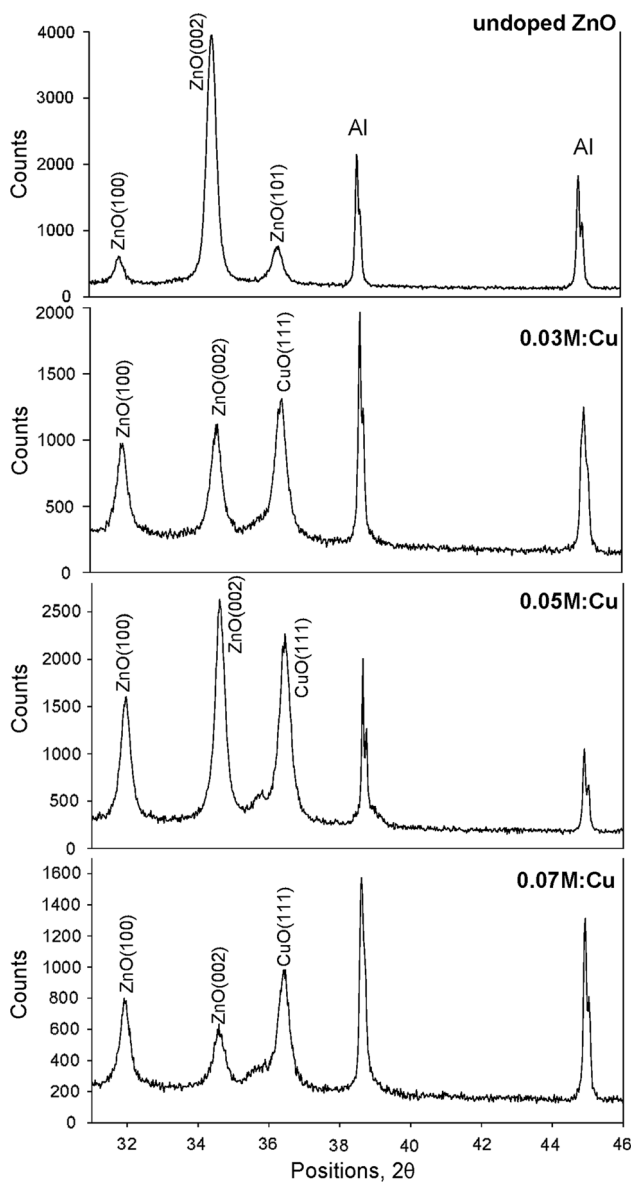


**Fig. 3** XRD spectra of undoped ZnO and Cu doped ZnO thin films

reported by Lee et al. [17] that had decreasing in intensity for peak (002). Formation of metallic cluster at high concentration of Cu is possible which could be obstacles the growth of nanorods. Besides, this can be related to the substitution of Cu ions having ionic radii of 0.57 Å for Zn ions having ionic radii of (0.64 Å) into the ZnO host lattice. The substitution leads to the creation of newer nucleation canters in the films which in turn change the nucleation type from homogenous to heterogeneous [18]. Even though this not main case in this study, the results clearly shown high concentration of Cu ions in the sol–gel solution could retard the growth of ZnO along (002) orientation. This indicates that few percentage of Cu doping into ZnO lattice could also affect the crystalline structure

of the film where it was observed CuO was found in all Cu doped samples with (111) orientation.

Literature reported that the lattice parameters of the host materials gets altered in the presence of dopant material due to their different atomic radii which the dopant may situate in the voids or can replace Zn ions in the host lattice. However, the basic structure of ZnO (wurtzite) remains the same, which signifies that most of the Cu ions go in the lattice as substitutional ions replacing the Zn ions instead of getting into void spaces [19]. Incorporated of  $\text{Cu}^{2+}$  ions into the ZnO crystal lattice might have little effect on lattice constant of ZnO since  $\text{Cu}^{2+}$  and  $\text{Zn}^{2+}$  ions have almost similar ionic radii. The c axis lattice values for (002) oriented Cu doped ZnO thin film were calculated using the following relation and the results are plotted as shown in Fig. 4. From the Fig. 4, it is observed that the c axis lattice constant shows decreasing trend from 5.2000 Å (undoped ZnO) to 5.183 Å (0.07 M:Cu) as the Cu concentration increases. This decrease in lattice value is only due to the ionic radii of Cu which is small as compared with that of Zn. As a result, the lattice contraction of doped ZnO is possible. It is considered that  $\text{Cu}^{2+}$  substitute  $\text{Zn}^{2+}$  and  $\text{Cu}^{2+}$  interstitial might be the main reasons because the lattice constant c was changed by these defects. Recently, Gonzalez et al. [20] reported the effect of Cu doping on c axis lattice constant of ZnO thin films and detected the decreasing behavior in c-orientation for Cu doping. Meanwhile, a small increase in c-axis lattice value could also be observed for higher Cu concentration (0.07 M:Cu) and it is agreed with the results reported by Lee et al. [17]. Besides that, Lee added moderate quantity of Cu could be considered to exist as interstitials that shared the oxygen with Zn atoms and hence improve the (002) orientation, but excess Cu-doping atoms can be energetically favorable to coalesce into metallic copper clusters and hence inhibit c-axis preferred growth of the ZnO film.

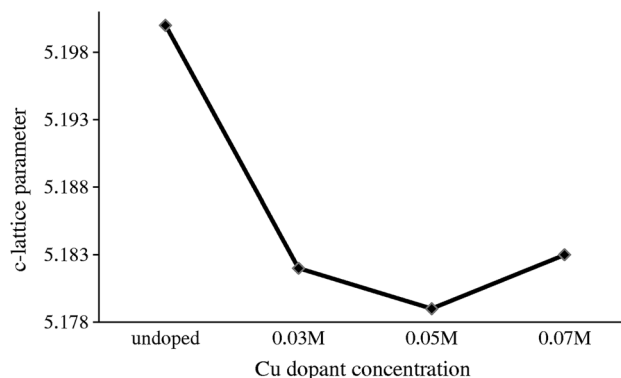


**Fig. 4** C-lattice parameter variation of (002) oriented Cu doped ZnO thin films

### 3.3 Surface morphological characterization of Cu doped ZnO

To study the surface behavior as a result of Cu doping, the surface morphology is recorded by FESEM and the images are displayed as given in Fig. 5. It has been detected from the Fig. 5b until Fig. 5d that the impurities such as CuO was also identified in all Cu doped samples that match with file JCPDS No.: 03-065-3288. Table 2 summarizes the details of CuO peak observed from the XRD analysis of doped ZnO thin film.

When Cu concentration increases, it is observed that, the position of (111) oriented peak is also changed where the trend of the values of FWHM and intensity are also increasing. However, when Cu doping concentration is increased to 0.05 M:Cu the intensity of peaks are enhanced again and the FWHM is decreased. This suggests the crystalline quality of ZnO thin film is greatly improved by 0.05 M:Cu. On the other hand, when Cu doping concentration is above 0.05 M:Cu the crystalline quality is weakened again indicated by reduction of peak intensity and FWHM. Although undoped ZnO (Fig. 5a) show

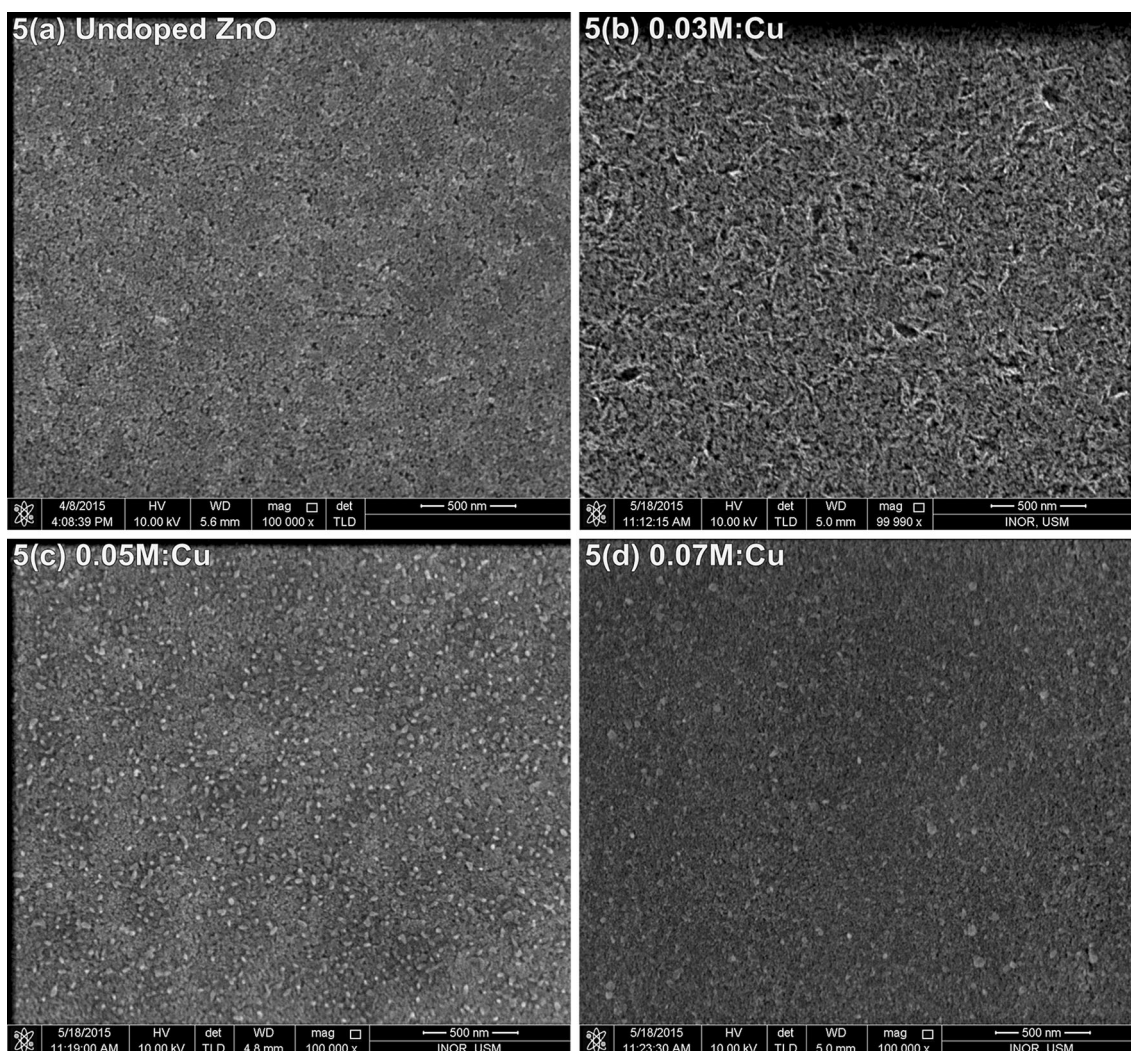


**Fig. 5** FESEM micrographs of **a** Undoped ZnO, **b** 0.03 M:Cu, **c** 0.05 M:Cu and **d** 0.07 M:Cu

**Table 2** The XRD data of (111) oriented ZnO thin film deposited on Al and Si substrates for different doping concentration

Cu doping	Orientation	Position ( $2\theta$ )	Intensity	FWHM ( $\beta$ )	Crystallite size [D (nm)]
0.03 M:Cu	111	36.407	1069.303	0.275	0.318
0.05 M:Cu	111	36.477	1928.118	0.234	0.373
0.07 M:Cu	111	36.454	801.404	0.157	0.556

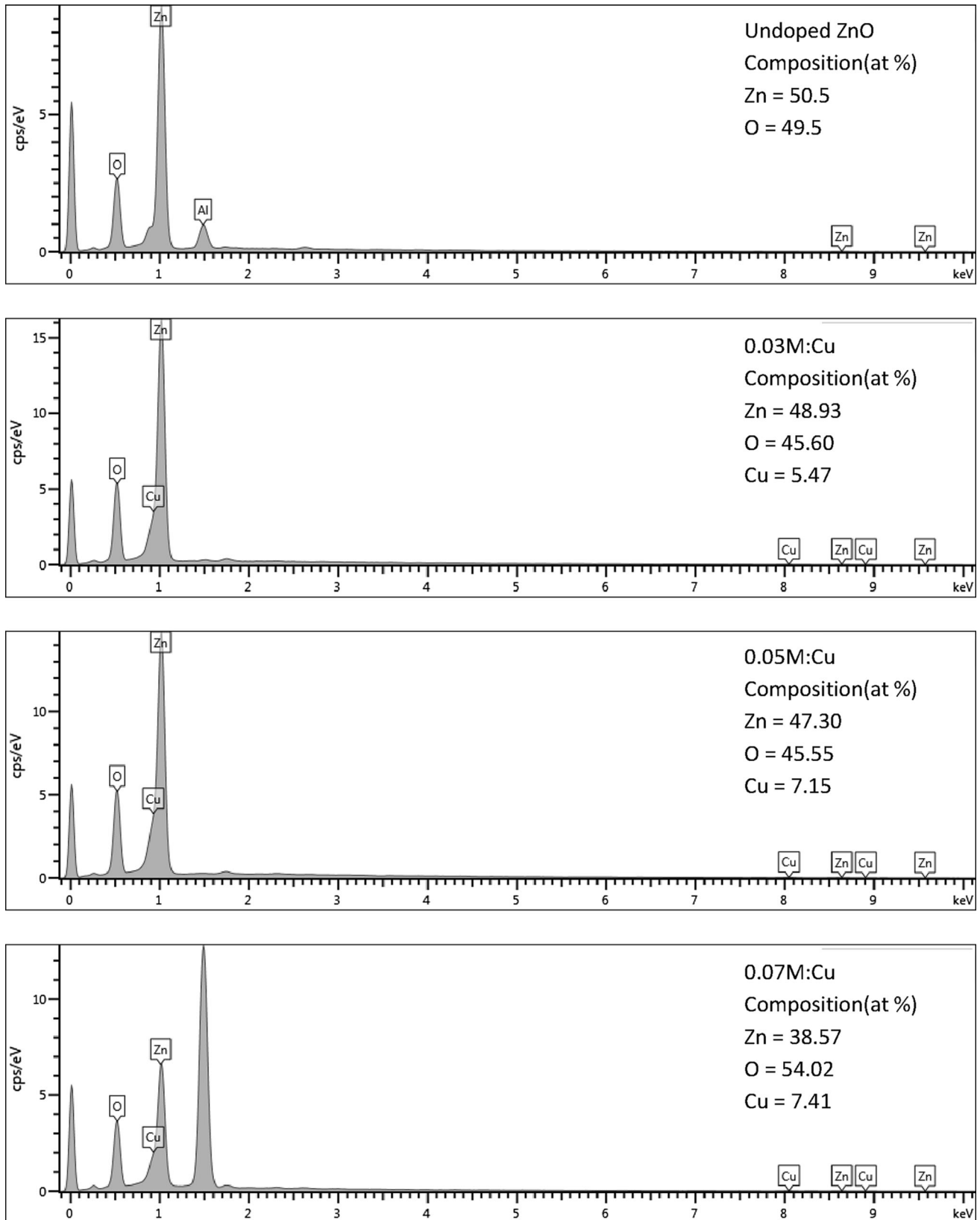
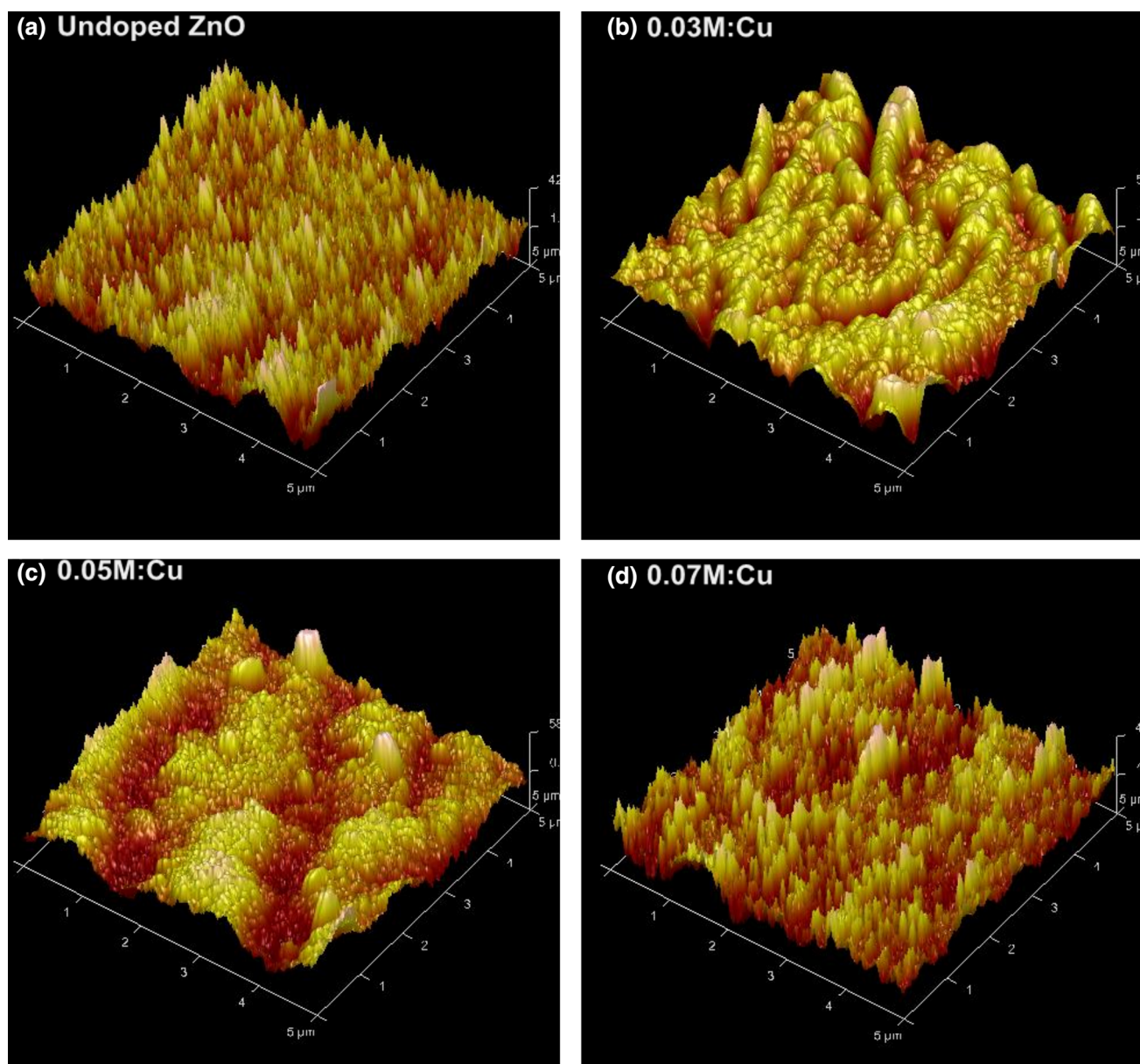


Fig. 6 EDS spectra of undoped ZnO and Cu doped ZnO thin films





**Fig. 7** AFM images of undoped ZnO and Cu doped ZnO thin films

**Table 3** Average surface roughness (Ra) and particle size of Cu doped ZnO thin film for various doping concentration

Sample	Surface roughness [Ra (nm)]	Particle size (nm)
Undoped ZnO	14.7	23
0.03 M:Cu	16.5	10
0.05 M:Cu	16.2	19
0.07 M:Cu	10.1	15

homogenous distribution of grains, a noticeable change in surface morphology of the doped ZnO films could be observed the Fig. 5b. From the analysis mentioned above, crystallization quality of the samples were degenerated gradually with the increase of Cu concentration. Crystallite

size belongs to doping concentration (0.03 M:Cu, 0.05 M:Cu, 0.07 M:Cu) was not significance with FESEM result (Fig. 5) where the films have smooth surface and comprising uniform grain size 51.18, 44.39, 27.84 nm as doping concentration increases. From Fig. 5, it can be deduced the microstructures of Cu doped ZnO thin films becomes homogeneous and closely packed at 0.07 M:Cu doping. This can be attributed that by increasing the dopant content, the grain size of thin films also decreased which then make the small grains no pores. Shukla also reported the improvement of thin films surface from holes and flakes structure to small needle-structure as [21]. In addition, it can be related to two possible reasons: (1) the increasing number of nucleation will lead the formation of small

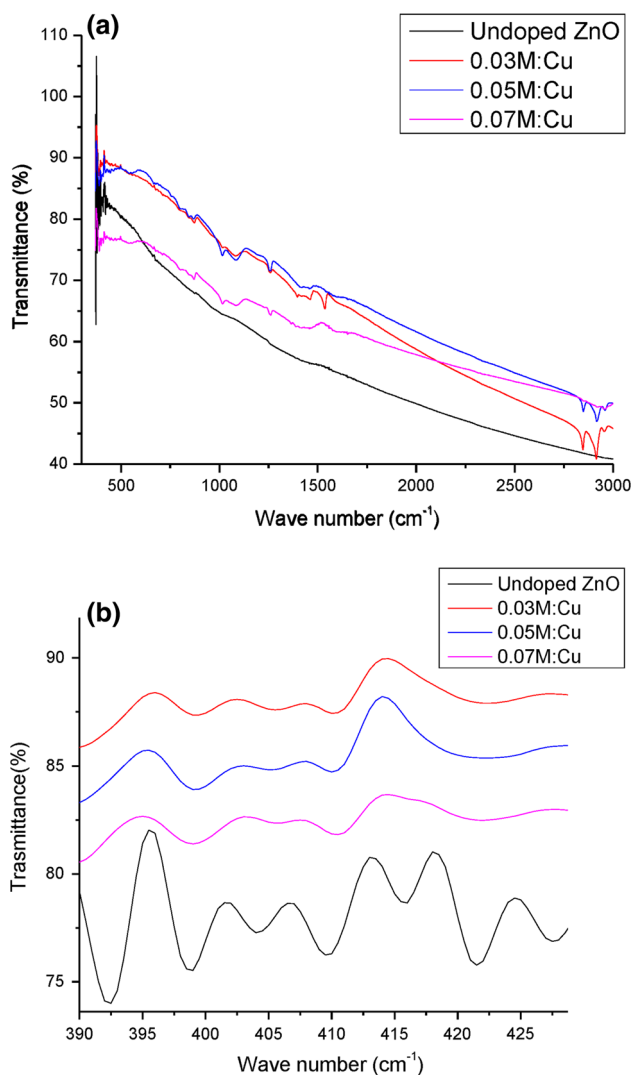


**Fig. 8** **a** FTIR spectra of undoped ZnO and Cu doped ZnO. **b** FTIR spectra in the range from 350 to 700  $\text{cm}^{-1}$

grains during incorporation of the dopant into the host material and (2) the disturbance of grain growth by stress might due to the difference in ion radius between zinc and aluminum [22]. Other than that, it might be due to high Cu concentration and also high annealing temperature for the process of thin film on metal substrates. EDS spectra of undoped ZnO and Cu doped ZnO are shown in Fig. 6. It can be distinguished Zn, Cu, O peaks from the Al substrates. The incorporation of Cu in Cu doped ZnO films was confirmed by EDX spectra. The figure clearly shows that when Cu dopant increased the Cu contents also increasing which shows the presence of Cu in this thin films.

In addition to FESEM analysis, the surface morphology of undoped and Cu doped ZnO thin film was processed using AFM and the recorded images are presented as shown in Fig. 7. It clearly shows the influence of Cu

doping on ZnO surface parameters. For better visualization, AFM was used to measure the surface roughness of the film by tapping mode. Using AFM software, the particle size was also evaluated and presented in Table 3. Both surface roughness and particle size are affected when ZnO is doped with Cu where the surface roughness increase when introduce with 0.03 M:Cu doping and suddenly decrease when there is increment amount of Cu doping in ZnO thin films. However, it was observed the changes in particle size are anomalous as the doping increase. The undoped ZnO thin film showed uniform grain growth compared with 0.03 M:Cu which form agglomeration due to presence of grains in different dimensions. For 0.05 M:Cu, it was observed smooth structure in certain area and non uniform height topography on the surface which caused more roughness compared with 0.07 M:Cu surface that showed close packed crystallite with voids that looks rougher which actually an uniform particles height. Increment in surface roughness from 14.7 (undoped ZnO) to 16.5 nm (0.03 M:Cu) is might due to major grain growth. The process of grain coalescence in doping might cause major grain growth that resulting in increasing porosity and surface roughness [23]. Types of substrates also affect the grains growth where epitaxial growth on Al substrates influenced the formation of wider grains of Cu doped ZnO. Kajikawa et al. [24] reported that the initial nucleation of polycrystalline films can depend on the type of substrate, and that the film growth can be epitaxial or non-epitaxial, which consequently influences the final morphology of the films. In addition, Wang et al. [25] showed the morphological differences of ZnO:Al thin film on various substrates such as glass substrates, polyamide and stainless steel at 300 °C. In this case, it was reported that the surface roughness was increased and grain size was decreased as compared to the values observed for the films deposited on stainless steel.

### 3.4 FTIR analysis

FTIR spectra spectroscopy is very useful tools for investigating vibrational properties of synthesized materials. The frequencies where absorption happens may indicate the type of functional group present in the substance. The band positions and absorption peak not only depend on the chemical composition and structure of the thin films but also on the morphology of thin films. FTIR transmittance spectra of undoped and Cu doped ZnO are recorded at room temperature as shown in Fig. 8. From the Fig. 8, it reveals the influence of metal doping on optical properties of ZnO thin films. As can be seen, for undoped ZnO, the observed intense absorption peak at  $\sim 410 \text{ cm}^{-1}$  is related to the stretching vibrations of Zn–O bond. The stretching

vibration around  $\sim 415\text{ cm}^{-1}$  belongs to TO mode of wurtzite ZnO and caused ZnO stretching vibration for tetrahedral surrounding of zinc atoms. The Zn–O bond is assigned to the stretching frequency at  $412\text{ cm}^{-1}$  for undoped ZnO which is shifted to higher frequency as  $416\text{ cm}^{-1}$  for 0.03 M Cu,  $415\text{ cm}^{-1}$  for 0.05 M Cu and  $414\text{ cm}^{-1}$  for 0.07 M Cu. Copper atom is slightly lighter than Zn atom, so, according to the theories of vibrational modes in mixed crystals, the substitution should result in an upward shift of the fundamental transverse optical phonon mode [26]. From here, the upward shift observed is in consistent with the results where the frequency of Zn–O is shifting to higher value when Cu doping is introduced. This phenomenon reveals the substitution of  $\text{Cu}^{2+}$  into the Zn–O lattice.

#### 4 Conclusions

Undoped ZnO and Cu doped ZnO thin films were successfully synthesized via sol–gel spin coating method on two different substrates. Influence of different annealing and different substrate on undoped ZnO was studied based on structural properties and the surface morphology. Undoped ZnO show finer and smooth surface topography with increasing crystallite size when annealed temperature increases. According to structural studies from the XRD analysis, all samples were polycrystalline and had hexagonal wurtzite structure. For doped ZnO, Cu doping that deposited on Al substrates shown the presence of CuO elements in XRD peaks and EDS spectra. For surface morphology of Cu doped ZnO, it was observed the increment trend values of crystallites size while surface roughness were anomalous when concentration is increasing. FTIR spectra shown shifting in higher frequency for Zn–O bond when Cu doping introduced to ZnO.

**Acknowledgments** The authors would like to thank for the FRGS project (203/PFIZIK/6711350) that provides the fund to carry out the research work successfully in school of physics. In addition, the authors would like to acknowledge for the use of research facilities such as spin coating machine, FESEM, FTIR etc., available in NOR Lab, School of Physics, Universiti Sains Malaysia.

#### References

1. S. Thakur, N. Sharma, A. Varkia, J. Kumar, *Adv. Appl. Sci. Res.* **5**, 18 (2014)
2. Y.W. Heo, D.P. Norton, S.J. Pearton, *J. Appl. Phys.* **98**, 073502 (2005)
3. S.T. Tan, B.J. Chen, X.W. Sun, *J. Appl. Phys.* **98**, 013505 (2005)
4. E. Bacaksiz, M. Parlak, M. Tomakin, A. Ozcelik, M. Karakiz, M. Altunbas, *J. Alloys Compd.* **466**, 447 (2008)
5. S.A. Kamaruddin, K.Y. Chan, H.K. Yow, M.Z. Sahdan, H. Saim, D. Knipp, *Appl. Phys. A* **104**, 263 (2011)
6. N. Nagarani, V. Vasu, *J. Photonics Spintron.* **2**, 19 (2013)
7. L. Dejam, S.M. Elahi, H.H. Nazari, H. Elahi, S. Solaymani, A. Ghaderi, *J. Mater. Sci. Mater. Electron.* (2015). doi:[10.1007/s10854-015-3804-7](https://doi.org/10.1007/s10854-015-3804-7)
8. S.B. Majumder, M. Jain, P.S. Dabal, R.S. Katiyar, *Mater. Sci. Eng. B* **103**, 16 (2003)
9. X. Feng, *J. Phys. Condens. Matter* **16**, 4251 (2005)
10. K. Laurent, D.P. Yu, S. Tusseau-Nenez, Y. Leprince-Wang, *J. Phys. D Appl. Phys.* **41**, 195410 (2008)
11. S.K. Pandey, S.K. Pandey, V. Awasthi, A. Kumar, U.P. Deshpande, M. Gupta, S. Mukherjee, *Bull. Mater. Sci.* **37**, 983 (2014)
12. K.S. Hwang, Y.J. Lee, S. Hwangboo, *J. Ceramic. Proc. Res.* **8**, 305 (2007)
13. M. Ashokkumar, S. Muthukumar, *J. Mater. Sci. Mater. Electron.* **25**, 398 (2014)
14. S.Y. Kuo, W.C. Chen, C.-P. Cheng, *Superlattices Microstruct.* **39**, 162 (2006)
15. I.W. Kim, S.J. Doh, C.C. Kim, J.H. Je, J. Tashiro, M. Yoshimoto, *Appl. Surf. Sci.* **241**, 179 (2005)
16. A.S. Gadallah, M.M. El-Nahass, *Adv. Condens. Matter Phys.* (2013). doi:[10.1155/2013/234546](https://doi.org/10.1155/2013/234546)
17. J.B. Lee, H.J. Lee, S.H. Seo, J.S. Park, *Thin Solid Films* **398**, 641 (2001)
18. V. Gupta, A. Mansingh, *J. Appl. Phys.* **80**, 1063 (1996)
19. P.D. Sahare, V. Kumar, *Int. J. Innov. Technol. Explor. Eng. (IJITEE)* **3**, 15 (2013)
20. A.E. Jimenez Gonzalez, *Solid State Chem.* **128**, 176 (1997)
21. R.K. Shukla, A. Srivastava, N. Kumar, A. Pandey, M. Pandey, *J. Nanotechnol.* (2015). doi:[10.1155/2015/172864](https://doi.org/10.1155/2015/172864)
22. J. Hu, R.G. Gordon, *J. Appl. Phys.* **71**, 880 (1992)
23. N.B. Ibrahim, S.M. Al-shomar, S.H. Ahmad, *Sains Malays.* **42**, 1781 (2013)
24. Y. Kajikawa, *J. Cryst. Growth* **289**, 387 (2006)
25. X. Wang, X. Zeng, D. Huang, X. Zhang, Q. Li, *J. Mater. Sci. Mater. Electron.* **23**, 1580 (2012)
26. D.W. Taylor, in *Optical Properties of Mixed Crystals*, ed. by R.J. Elliott, I.P. Ipatova (North Holland, Amsterdam, 1988), p. 35